Redox Properties of Cytochrome *c* Adsorbed on Self-Assembled Monolayers: A Probe for Protein Conformation and Orientation

Xiaoxi Chen, Rosaria Ferrigno, Jerry Yang, and George M. Whitesides*

Department of Chemistry and Chemical Biology, Harvard University, 12 Oxford Street, Cambridge, Massachusetts 02138

Received May 21, 2002

The redox behavior of cytochrome *c* (cyt *c*) adsorbed to gold electrodes modified with self-assembled monolayers (SAMs) depends on the SAM. This paper examines SAMs generated from alkanethiols terminating in trimethylammonium (**1**), sulfonate (**2**), methyl (**3**), amine (**4**), and carboxylic acid (**5**) groups and from an aromatic thiol (**6**). The redox potentials of cyt *c* adsorbed on SAMs of **1** and **5** are relatively close to the formal potential of native cyt *c* measured in solution. The redox potentials of cyt *c* adsorbed on SAMs of **3**, **4**, and **6** are significantly shifted from the formal potential, and a reduction peak at about 0.5 V more negative than the formal potential (that is, a value corresponding to a more difficult reduction) was observed in all three cases. These observations suggest that cyt *c* changes its conformation significantly on adsorption on these surfaces. No redox peaks were observed for cyt *c* adsorbed on SAMs of **2**, although surface plasmon resonance (SPR) studies indicate that the SAMs of **2** irreversibly adsorbed approximately a double layer of cyt *c*. Mixed SAMs were also studied. Most interestingly, cyt *c* adsorbed on mixed SAMs formed from the combinations of **1** and **2** exhibited significantly slower electron transfer (0.3−1.2 s^{-1}) than cyt *c* adsorbed on a homogeneous SAM of **1** (45 s^{-1}). These observations suggest changes in protein orientation due to the presence of the sulfonate groups at the interface. This study suggests that electrochemical measurement can be a useful probe for the conformation and orientation of protein adsorbed on surfaces.

Introduction

Understanding the orientation and conformation of proteins adsorbed on solid surfaces is important in the design of biomaterials, biosensors, and bioanalytical systems.[1,2] Among the factors that determine orientation and conformation is the molecular structure of the surface. Self-assembled monolayers (SAMs) have become universal tools with which to study the relations between the structures and properties of organic surfaces and their influence on protein adsorption.[3−7] Here, we have examined the conformational and orientational characteristics of a well-characterized, redox-active metalloprotein—cytochrome *c* (cyt *c*)—adsorbed on the interface of SAM-modified gold electrodes. We have used the redox properties of the heme (iron protoporphyrin IX) moiety embedded in cyt *c* as one measure of protein conformation and orientation. Redox behavior—the rate and potential of electron transfer from the electrode supporting the SAM to/from the heme—is not information-rich and does not yield detailed information about the structure of the protein, but it is easily measured in proteins adsorbed at monolayer coverages and it provides a qualitatively interpretable sensor for conformation and/or orientation.

Horse heart cytochrome *c* (Figure 1), a relatively simple metalloprotein comprising only 104 amino acids, is often used as the prototypical metalloprotein from a structural point of view.[8] Studies of its electrochemistry have, however, been hampered because it adsorbs strongly on Pt, Hg, Au, Ag, and other electrodes; this adsorption has been shown to result in large changes in its conformation and often in denaturation of the protein.[9−12] Efforts to limit denaturing adsorption have led to the use of SAMs to modify the electrode surface.[8,13,14]

This work had two objectives: one practical and one mechanistic. The practical objective was, using an appropriate choice of SAM, to minimize the level of "destructive" adsorption—that is adsorption resulting in denaturation—of cyt *c* on the surface of an electrode and to make it possible to prepare cyt *c* in an adsorbed form that allowed rapid exchange of electrons between the protein and an electrode. Choosing a SAM for this purpose required a balance: If the interaction between the surface and the protein were weak, conformational changes in the protein might be limited but adsorption would be incomplete; if the interaction were strong, adsorption would be complete but the protein might denature on the surface. In addition, interaction between the surface and the protein should be specific enough to induce the protein to sit on the surface in an orientation that allowed rapid electron transfer. The heme edge of cyt *c* must be close to the electrode surface for electron exchange[8] to be fast.

* To whom correspondence should be addressed. E-mail: gwhitesides@gmwgroup.harvard.edu.

(1) Zhang, S.; Wright, G.; Yang, Y. *Biosens. Bioelectron.* **2000**, *15*, 273−282.
(2) Brockman, J. M.; Nelson, B. P.; Corn, R. M. *Annu. Rev. Phys. Chem.* **2000**, *51*, 41−63.
(3) Whitesides, G. M. *Chimia* **1990**, *44*, 310−311.
(4) Laibinis, P. E.; Bain, C. D.; Nuzzo, R. G.; Whitesides, G. M. *J. Phys. Chem.* **1995**, *99*, 7663−7676.
(5) Mrksich, M.; Whitesides, G. M. *Annu. Rev. Biophys. Biomol. Struct.* **1996**, *25*, 55−78.
(6) Wink, T.; Zuilen, S. J. v.; Bult, A.; Bennekom, W. P. v. *Analyst* **1997**, *122*, R43−R50.
(7) Tengvall, P.; Lundstrom, I.; Liedberg, B. *Biomaterials* **1998**, *19*, 407−422.
(8) Fedurco, M. *Coord. Chem. Rev.* **2000**, *209*, 263−331.
(9) Hinnen, C.; Parsons, R.; Nikki, K. *J. Electroanal. Chem.* **1983**, *147*, 329−337.
(10) Reed, D. E.; Hawkridge, F. M. *Anal. Chem.* **1987**, *59*, 2334−2339.
(11) Hawkridge, F. M.; Taniguchi, I. *Comments Inorg. Chem.* **1995**, *17*, 163−187.
(12) Armstrong, F. A. *Struct. Bonding* **1990**, *72*, 137−230.
(13) Allen, P. M.; Hill, H. A. O.; Walton, N. J. *J. Electroanal. Chem.* **1984**, *178*, 69−86.
(14) McLendon, G. *Acc. Chem. Res.* **1988**, *21*, 160−167.

10.1021/la0204794 CCC: $22.00
Published on Web 08/03/2002

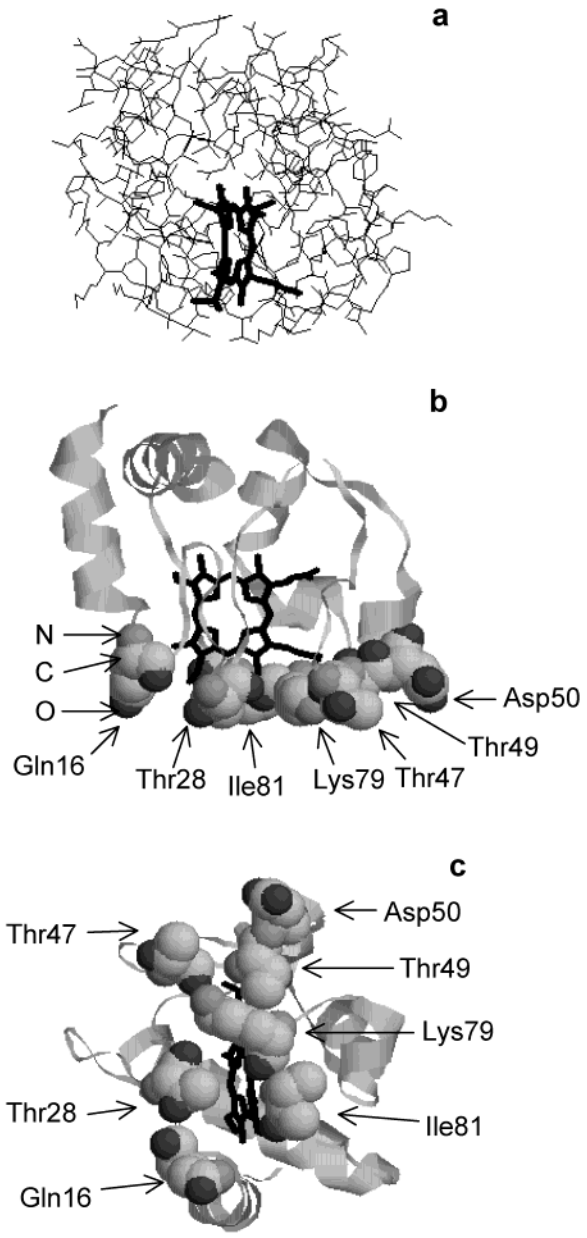

Figure 1. RASMOL presentations of the crystal structure of horse heart cytochrome *c* (Protein Database, http://www.rcsb.org/pdb/, file "1HRC"). (a) The amino acids are shown in thin lines, and the heme group is shown in thick lines. (b) The protein backbone is shown in ribbons, and the heme group is shown in thick lines (the iron atom at the center of the heme group is not shown). The figure also picks out the surface residues that are close to the heme group and presents in a space-filling model. (c) Same as (b), shown in another orientation.

Since electron transfer occurs by tunneling, and since electron-transfer rates decrease exponentially with the distance between the heme and the surface of electrode, slight deviations from an optimal orientation have the potential to cause the rates of electron-transfer rate to decrease significantly. For example, assuming an exponential decrease of the rate of electron transfer with distance and a value of $\beta = 14$ nm^{-1} (rate $\propto e^{-\beta d}$, where d is the electron-transfer distance) through an average protein matrix,[15,16] an increase in distance of 0.5 nm will cause the electron-transfer rate to slow by a factor of $\sim 10^3$. A large decrease in the rate of electron transfer would quickly cause the redox reactions involving the adsorbed protein to become unobservable using conventional electrochemical measurements.

The second mechanistic objective was to develop an easily interpreted measure of the conformation of a protein adsorbed on the surface of SAMs. We have examined the adsorption of proteins on SAMs extensively and have developed a good qualitative understanding of the relationship between the molecular structure of molecules making up the SAM and the tendency of the SAM to adsorb protein. In cases where protein adsorbs, however, we have very little information concerning *conformation*. We hoped that the redox properties of cyt *c* might provide a low-resolution but easily interpreted measure of conformation. Since the rate of electron transfer to and from the heme is very sensitive to distance and conformation, studies of *rates* of electron transfer would suggest the geometry of the heme relative to the surface of the electrode. The potential at which electron transfer occurs correspondingly provides a measure of the environment of the heme moiety.

Recent studies indicate that carboxyl-terminated SAMs formed from thiols of structure $HS(CH_2)_nCOOH$ ($n = 2-16$) allow reversible or quasi-reversible cyclic voltammetry of adsorbed horse-heart and yeast cyt *c*.[17−21] It is widely believed that the negatively charged carboxyl-terminated SAMs cause the lysine-rich, positively charged (at neutral pH) cyt *c* to adsorb on the surface with a relatively unperturbed structure and to adopt an orientation with respect to the electrode that permits rapid electron exchange.[8] In this study, we surveyed several SAMs with a range of surface properties for their effect on the conformation and orientation of cyt *c*. We chose SAMs terminating in $N^+(CH_3)_3$ and SO_3^- groups to represent charged surfaces, SAMs terminating in COOH and NH_2 groups to provide pH-dependent, charged surfaces (that is, surfaces whose charge depended on the protonation state of the acidic/basic groups) and surfaces capable (over some ranges of potential) of extensive hydrogen bonding, and SAMs terminating in methyl and phenyl groups to provide hydrophobic surfaces. We chose a tris(ethylene glycol)- ($(EG)_3OH$-) terminated SAM—a type of SAM that has been established to resist protein adsorption[22−28]—to serve as a control. We also studied mixed SAMs to clarify details of the effect of surface properties on the conformation and orientation of the adsorbed cyt *c*.

Results and Discussion

Preparation of SAMs and Conditions for Protein Adsorption. Evaporating a thin layer of gold (40 nm)

(15) Moser, C. C.; Keske, J. M.; Warncke, K.; Farid, R. S.; Dutton, P. L. *Nature* **1992**, *355*, 796−802.
(16) Page, C. C.; Moser, C. C.; Chen, X.; Dutton, P. L. *Nature* **2000**, *402*, 47−52.
(17) Tarlov, M. J.; Bowden, E. F. *J. Am. Chem. Soc.* **1991**, *113*, 1847−1849.
(18) Song, S.; Clark, R. A.; Bowden, E. F.; Tarlov, M. J. *J. Phys. Chem.* **1993**, *97*, 6564−6572.
(19) Arnold, S.; Feng, Z. Q.; Kakiuchi, K.; Knoll, W.; Niki, K. *J. Electroanal. Chem.* **1997**, *438*, 91−97.
(20) Kasmi, A. E.; Wallace, J. M.; Bowden, E. F.; Binet, S. M.; Linderman, R. J. *J. Am. Chem. Soc.* **1998**, *120*, 225−226.
(21) Clark, R. A.; Bowden, E. F. *Langmuir* **1997**, *13*, 559−565.
(22) Prime, K. L.; Whitesides, G. M. *Science* **1991**, *252*, 1164−1167.
(23) Prime, K. L.; Whitesides, G. M. *J. Am. Chem. Soc.* **1993**, *115*, 10714−10721.
(24) Ostuni, E.; Yan, L.; Whitesides, G. M. *Colloids Surf., B* **1999**, *15*, 3−30.
(25) Kingshott, P.; Griesser, H. J. *Curr. Opin. Solid State Mater. Sci.* **1999**, *4*, 403−412.
(26) Chapman, R. G.; Ostuni, E.; Liang, M. N.; Meluli, G.; Kim, E.; Yan, L.; Pier, G.; Warren, H. S.; Whitesides, G. M. *Langmuir* **2001**, *17*, 1225−1233.
(27) Chapman, R. G.; Ostuni, E.; Takayama, S.; Holmlin, R. E.; Yan, L.; Whitesides, G. M. *J. Am. Chem. Soc.* **2000**, *122*, 8303−8304.
(28) Luk, Y. Y.; Kato, M.; Mrksich, M. *Langmuir* **2000**, *16*, 9604−9608.

onto glass microscope slides that had been primed with an adhesion layer of titanium (1 nm) provided chips for measurements using both electrochemistry and SPR spectroscopy. SAMs formed on the gold films upon soaking them in 2 mM solutions of the appropriate thiol (or mixture of thiols) in ethanol or water for ~24 h. The characterization of SAMs of $S(CH_2)_{11}N^+(CH_3)_3$ and $S(CH_2)_{11}SO_3^-$ by ellipsometry and contact angle measurements has been reported previously.[29] SAMs of $S(CH_2)_{11}CH_3$, $S(CH_2)_{10}COOH$, $S(CH_2)_{11}NH_2$, and $S(CH_2)_{11}(EG)_3OH$ have also been studied previously.[23,30−33]

For electrochemical measurements, we immersed the SAM-coated chip in a solution of cyt *c* (1 mg/mL) in phosphate buffer (pH 7.0, ionic strength $\mu = 1$ mM) for 30 min. The chip was then rinsed with buffer and assembled in a three-electrode electrochemical cell filled with an electrolyte (phosphate buffer, pH 7.0, $\mu = 10$ mM) free of the protein. Before the electrochemical measurements started, the chip was equilibrated in the cell for 5−10 min while the electrolyte was purged with Ar.

For SPR,[34,35] we allowed the solution of cyt *c* (the same as that used in the electrochemical measurements) to flow over the SAM on gold for 30 min. Protein adsorption was monitored as a function of time. We then allowed a buffer—which is equivalent to the electrolyte solution in the electrochemical measurements—to flow over the chip for 10 min. The amount of protein adsorbed was measured in response units (RU; 10 000 RU correspond to a shift of 1° in the angle of incidence of light that excites surface plasmons in the gold). We report values of ΔRU, which is the change in RU relative to the response for the clean surface exposed to buffer without protein ($\Delta RU = RU^{buffer+protein} - RU^{buffer}$).

Redox Properties of Cyt *c* Adsorbed on Homogeneous SAMs. *SAM of $S(CH_2)_{11}N^+(CH_3)_3$.* We observed voltammetric peaks due to adsorbed cyt *c* on the SAM of $S(CH_2)_{11}N^+(CH_3)_3$ (Figure 2a). The redox potential of cyt *c*, taken as the average of the reduction and oxidation peak potential, is 0.13V vs Ag/AgCl.

The formal redox potential for the ferri/ferro-cyt *c* couple, measured in neutral solution of pH 7, is 0.07 V vs Ag/AgCl (pH 7) and changes with temperature,[36−38] pressure,[39,40] electrolyte composition, and ionic strength.[41,42] The redox potential of cyt *c* adsorbed on the SAM of $S(CH_2)_{11}N^+(CH_3)_3$, when measured at low ionic strength ($\mu = 10$ mM) and pH 7, is about 0.06 V higher (easier to reduce) than the formal redox potential. The small potential shift relative to the formal potential can be rationalized in terms of the effect of the positive charges of the $N^+(CH_3)_3$ groups close to the heme pocket on the potential. The influence of buffer, temperature, and other details of the experiment may also contribute.

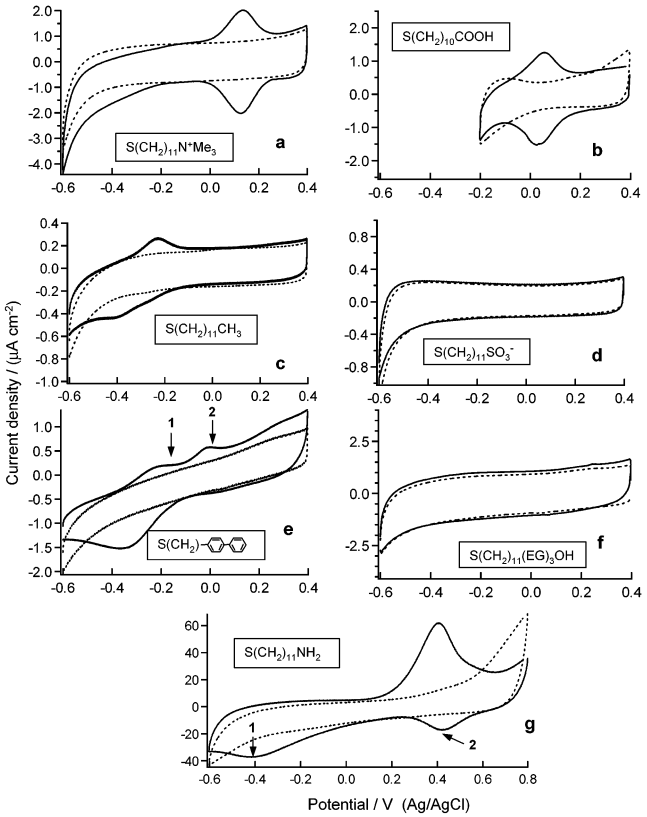

Figure 2. Cyclic voltammograms of horse heart cyt *c* adsorbed on homogeneous SAMs of (a) $S(CH_2)_{11}N^+(CH_3)_3$, (b) $S(CH_2)_{10}COOH$, (c) $S(CH_2)_{11}CH_3$, (d) $S(CH_2)_{11}SO_3^-$, (e) $S(CH_2)(C_6H_4)(C_6H_5)$, (f) $S(CH_2)_{11}(OCH_2CH_2)_3OH$, and (g) $S(CH_2)_{11}NH_2$. The voltammetric scan rate is 0.1 V/s in a−f and is 1 V/s in g. Dashed lines represent background cyclic voltammograms of the corresponding SAM-modified electrode before exposing to cyt *c* solution for adsorption.

By integration of the peaks observed in cyclic voltammetry, we measured the amount of adsorbed cyt *c* that was electroactive and contributed to faradaic charge-transfer reactions. The analysis gave a surface coverage of electroactive cyt *c* as 16 pmol cm^{-2} on the SAM of $S(CH_2)_{11}N^+(CH_3)_3$. This value is close to the theoretical maximum coverage (15 pmol cm^{-2}) estimated on the basis of the crystal structure of cyt *c* and suggests there is a full monolayer coverage.[43] The cathodic-to-anodic peak separation is small (0.01 V) at a 0.1 V/s scan rate; this separation indicates that electron transfer is relatively rapid. This rate will be discussed in detail in the section on the mixed monolayer.

SAM of $S(CH_2)_{10}COOH$. We observed voltammetric peaks due to cyt *c* adsorbed on a SAM of $S(CH_2)_{10}COOH$ (Figure 2b). The average of the reduction and oxidation peak potential gave a redox potential as 0.04 V vs Ag/AgCl. Integration of the peaks gave a surface coverage of electroactive cyt *c* as 10 pmol cm^{-2}. The cathodic-to-anodic peak separation is 0.02 V at a 0.1 V/s scan rate. These parameters are similar to those reported in the literature.[17−21] The redox potential of cyt *c* adsorbed on the SAM of $S(CH_2)_{10}COOH$ is about 0.03 V lower than the

(29) Holmlin, R. E.; Chen, X.; Chapman, R. G.; Takayama, S.; Whitesides, G. M. *Langmuir* **2001**, *17*, 2841−2850.
(30) Bain, C. D.; Troughton, E. B.; Tao, Y.-T.; Evall, J.; Whitedes, G. M.; Nuzzo, R. G. *J. Am. Chem. Soc.* **1989**, *111*, 321−335.
(31) Nuzzo, R. G.; Dubois, L. H.; Allara, D. L. *J. Am. Chem. Soc.* **1990**, *112*, 558−569.
(32) Dubois, L. H.; Zegarski, B. R.; Nuzzo, R. G. *J. Am. Chem. Soc.* **1990**, *112*, 570−579.
(33) Lee, T. R.; Carey, R. I.; Biebuyck, H. A.; Whitesides, G. M. *Langmuir* **1994**, *10*, 741−749.
(34) Lofas, S.; Malmqvist, M.; Ronnberg, I.; Stenberg, E.; Liedberg, B.; Lundstrom, I. *Sens. Actuators, B* **1991**, *5*, 79−84.
(35) Mrksich, M.; Sigal, G. B.; Whitesides, G. M. *Langmuir* **1995**, *11*, 4383−4385.
(36) Yuan, X. L.; Hawkridge, F. M.; Chlebowski, J. F. *J. Electroanal. Chem.* **1993**, *350*, 29−42.
(37) Cai, C.-X.; Hu, H. X.; Chen, H. Y. *Electrochim. Acta* **1995**, *40*, 1109−1112.
(38) Battistuzzi, G.; Borsari, M.; Sola, M.; Francia, F. *Biochemistry* **1997**, *36*, 16247−16258.
(39) Cruanes, M. T.; Rodgers, K. K.; Sligar, S. G. *J. Am. Chem. Soc.* **1992**, *114*, 9660−9661.
(40) Sun, J.; Wishart, J. F.; Eldik, R. v.; Shalderes, R. D.; Swaddle, T. W. *J. Am. Chem. Soc.* **1995**, *117*, 2600−2605.
(41) Szucs, A.; Novak, M. *J. Electroanal. Chem.* **1995**, *383*, 75−84.
(42) Allen, H.; Hill, O.; Hunt, N. I.; Bond, A. M. *J. Electroanal. Chem.* **1997**, *436*, 17−25.

(43) We model cyt *c* molecule approximately as a solid sphere of 3.3 nm diameter, based on its crystal structure.

formal redox potential. This potential shift is in the direction opposite to that of cyt *c* adsorbed on the positively charged SAM of $S(CH_2)_{11}N^+(CH_3)_3$. This shift can plausibly be rationalized in terms of the effect of the negative charges of the COO^- groups close to heme pocket of cyt *c* on the potential.

The cyclic voltammogram shown in Figure 2b covers the range of potentials between −0.2 and 0.4 V. When the scan range was extended to below −0.2 V, the cyclic voltammogram of the SAM of $S(CH_2)_{10}COOH$ (without any protein adsorbed) is complicated by a pair of peaks corresponding to protonation and deprotonation of the surface COOH groups. The protonation and deprotonation peaks of surface COOH groups have been studied theoretically[44,45] and experimentally.[46]

SAM of $S(CH_2)_{11}CH_3$. We observed peaks in cyclic voltammetry due to cyt *c* adsorbed on a SAM of $S(CH_2)_{11}CH_3$ (Figure 2c). The reduction potential is −0.32 V vs Ag/AgCl. This value is about 0.4 V lower than the formal potential. The large potential shift suggests that cyt *c* changes conformation substantially on adsorption. One possible interpretation of these potentials is that cyt *c* denatures on the hydrophobic surface of the $S(CH_2)_{11}CH_3$ SAM and that the heme group is no longer well protected by the protein matrix and therefore more difficult to reduce than in the native conformation. The reduction potential of the heme observed here is indeed similar to that observed for heme molecules in water at neutral pH.[47]

A similar potential shift has been reported for denatured cyt *c*.[48] In that study, the redox potentials were measured for cyt *c* in solution using a gold electrode modified with 4,4′-bipyridine; this electrode is claimed not to induce strong adsorption of cyt *c*.[49] When guanidine hydrochloride (Gnd-HCl) was added to denature cyt *c* in solution, the redox potential shifted 0.45 V in the negative direction. Ferri et al.[48] also observed a distinct species whose redox potential lay between that of the native protein and the completely denatured protein when the concentration of Gnd-HCl is in the intermediate range. This species with intermediate potential will be further discussed in the section (below) dealing with an aromatic thiol.

SAM of $S(CH_2)_{11}SO_3^-$. There are no observable voltammetric peaks within the voltage window from −0.6 to +0.4 V vs Ag/AgCl for a system that ostensibly consists of cyt *c* adsorbed on SAMs of $S(CH_2)_{11}SO_3^-$ (Figure 2d). There are two possible explanations for the absence of voltammetric peaks: (1) There is no cyt *c* adsorbed on the surface. (2) There is adsorbed cyt *c*, but the heme groups in the protein are not electroactive or the electron transfer is very slow.

Surface Plasmon Resonance Spectroscopy. To quantify the total amount of adsorbed cyt *c* on the SAMs, we used surface plasmon resonance (SPR), using the *same* adsorption conditions (protein buffer, wash buffer, incubation time, and wash time) as those used to prepare the electrodes with adsorbed protein for the electrochemistry experiments. The mass of protein irreversibly adsorbed on the surface per unit area, Γ_{ir}, can be determined from

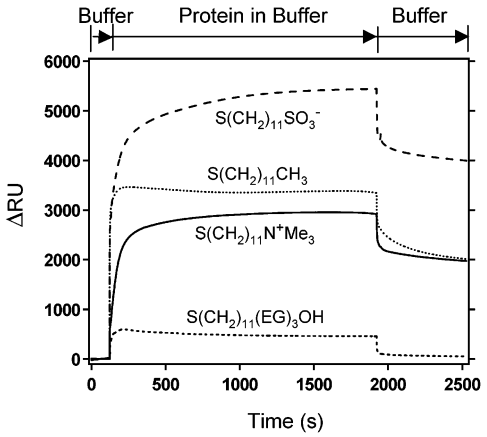

Figure 3. Plots of SPR response ΔRU as a function of time for the adsorption of cyt *c* to homogeneous SAMs of $S(CH_2)_{11}N^+(CH_3)_3$, $S(CH_2)_{11}CH_3$, $S(CH_2)_{11}SO_3^-$, and $S(CH_2)_{11}(OCH_2CH_2)_3OH$. The SAM that corresponds to each curve is defined on the plots. The curves for each protein flowing over the different SAMs were adjusted vertically to have the same value of ΔRU at the time when the solution containing the protein began to flow over the SAM. The region of time during which protein was present in the buffer is indicated above the plot.

ΔRU_{ir} using eq 1,[50,51] where ΔRU_{ir} is the ΔRU value at the end of the 10-min buffer wash.

$$\Gamma_{ir} = 0.09\ (ng/cm^2) \times \Delta RU_{ir} \qquad (1)$$

Figure 3 shows sensorgrams for the adsorption of cyt *c* to SAMs of $S(CH_2)_{11}N^+(CH_3)_3$, $S(CH_2)_{11}SO_3^-$, $S(CH_2)_{11}CH_3$, and $S(CH_2)_{11}(EG)_3OH$. The values of ΔRU found for the SAMs of $S(CH_2)_{11}N^+(CH_3)_3$ and $S(CH_2)_{11}CH_3$ are both approximately 2000 units. By applying eq 1, we obtained 180 ng/cm^2, or 14.5 pmol/cm^2, of cyt *c* irreversibly adsorbed on both SAMs. This value is consistent with both the surface coverage obtained from electrochemical analysis and the theoretical maximum surface coverage for a densely packed monolayer of protein. We therefore interpret $\Delta RU_{ir} = 2000$ as a full monolayer of cyt *c* irreversibly adsorbed.

Although the ΔRU found for cyt *c* adsorbed on the $S(CH_2)_{11}CH_3$ SAM suggests a full monolayer of adsorbed cyt *c*, integration of the voltammetric peaks indicates the surface coverage of electroactive cyt *c* to be 3.0 pmol cm^{-2}. This observation suggests that only about 20% of the adsorbed molecules are electroactive. This result can be rationalized by assuming random orientation of the denatured cyt *c* on the surface: only some orientations allow the heme edge to be close enough to the surface to allow significant electron exchange with the electrode.

The ΔRU value found for the SAMs of $S(CH_2)_{11}SO_3^-$ is approximately 4000; we interpret this value to mean that a *bilayer* of cyt *c* adsorbs on this surface. Even though a large amount of cyt *c* is adsorbed on the surface, either none of it is electroactive or the rate of electron transfer is unobservably slow. We hypothesize that the cyt *c* is not randomly oriented on the surface of the $S(CH_2)_{11}SO_3^-$ SAM but rather confined to "preferred" orientations—perhaps controlled by the strong electrostatic interactions between the surface and the protein—that place the heme group too far from the surface of the electrode to engage in electron transfer. While SAMs of $S(CH_2)_{10}COOH$ and

(44) Smith, C. P.; White, H. S. *Langmuir* **1993**, *9*, 1−3.
(45) Fawcett, W. R.; Fedurco, M.; Kovacova, Z. *Langmuir* **1994**, *10*, 2403−2408.
(46) White, H. S.; Peterson, J. D.; Cui, Q.; Stevenson, K. J. *J. Phys. Chem. B* **1998**, *102*, 2930−2934.
(47) Pilloud, D. L.; Chen, X.; Dutton, P. L.; Moser, C. C. *J. Phys. Chem. B* **2000**, *104*, 2868−2877.
(48) Ferri, T.; Poscia, A.; Ascoli, F.; Santucci, R. *Biochim. Biophys. Acta* **1996**, *1298*, 102−108.
(49) Eddows, M. J.; Hill, H. A. O. *J. Am. Chem. Soc.* **1979**, *101*, 4461−4464.
(50) Sigal, G. B.; Mrksich, M.; Whitesides, G. M. *J. Am. Chem. Soc.* **1998**, *120*, 3464−3473.
(51) The original equation was expressed in terms of the shift of the angle of incidence of light that excites surface plasmons (ΔΘ), where 10 000 RU correspond to ΔΘ = 1°.

$S(CH_2)_{11}N^+(CH_3)_3$ adsorb cyt *c* in orientations that allow the heme edge to be close enough to the surface of the electrode for electron transfer to occur at a kinetically significant rate, the SAM of $S(CH_2)_{11}SO_3^-$ apparently does not.

SAM of $S(CH_2)(C_6H_4)(C_6H_5)$. We observed one reduction peak and two oxidation peaks due to the adsorbed cyt *c* on the SAM of the aromatic thiol 4-(mercaptomethyl)-biphenyl (Figure 2e). This result suggests that there are at least two species of adsorbed molecules of cyt *c*. The positions of the reduction peak and one of the oxidation peaks (labeled "1" in Figure 2e) are similar to those observed for the SAM of $S(CH_2)_{11}CH_3$, and the position of the other oxidation peak (labeled "2" in Figure 2e) coincides with the potential of the partially unfolded species reported by Ferri et al.[48]

As with the SAM of $S(CH_2)_{11}CH_3$, we suggest that cyt *c* denatured on the hydrophobic surface of the aromatic SAM. With the aromatic SAM, however, it seems that two denatured conformations of cyt *c* form. One of them is completely denatured and produced the more negative oxidation peak (labeled "1" in Figure 2e); the other is an intermediate structure of presently undefined orientation and conformation and produced the more positive oxidation peak (labeled "2" in Figure 2e).

SAM of $S(CH_2)_{11}(OCH_2CH_2)_3OH$. We observed no peaks in the cyclic voltammogram of the $S(CH_2)_{11}(EG)_3OH$ SAM after the cyt *c* adsorption procedure (Figure 2f). This result is consistent with SPR results (Figure 3) that suggest that no cyt *c* molecules adsorb irreversibly to this surface.

SAM of $S(CH_2)_{11}NH_2$. We observed two reduction peaks and one oxidation peak due to cyt *c* adsorbed on the $S(CH_2)_{11}NH_2$ SAM (Figure 2g). The position of one of the reduction peaks (labeled "1" in Figure 2g) is close to the potential of the reduction peak observed for both the $S(CH_2)_{11}CH_3$ SAM and the aromatic SAM. The other reduction peak (labeled "2" in Figure 2g) is more positive than the standard potential; the corresponding oxidation peak is also more positive than the standard potential. The reduction peak labeled "1" in Figure 2g probably has the same origin as the reduction peaks in Figure 2c and e, that is, denatured cyt *c*. We do not understand the origin of the reduction peak labeled "2" and the single oxidation peak. The surface amine groups, if protonated and positively charged, may induce positive potential shifts of the heme groups.

Redox Properties of Cyt *c* Adsorbed on Mixed SAMs. On the basis of the electrochemical response of cyt *c* adsorbed on the homogeneous SAMs, we hypothesized that the CH_3-terminated SAM denatured the protein, the SO_3^--terminated SAM promoted a protein orientation unfavorable for electron transfer, and the $N^+(CH_3)_3$-terminated SAM both preserved the native structure of cyt *c* and promoted a protein orientation favorable for electron transfer. To explore this hypothesis, we studied two systems of mixed SAMs: (i) mixed SAMs of $S(CH_2)_{11}N^+(CH_3)_3$ and $S(CH_2)_{11}SO_3^-$, in which we hoped to see the transition between the "favorable" and "unfavorable" orientations; (ii) mixed SAMs of $S(CH_2)_{11}N^+(CH_3)_3$ and $S(CH_2)_{11}CH_3$, in which we hoped to see the transition between the native and denatured conformations.

Mixed SAMs of $S(CH_2)_{11}N^+(CH_3)_3$ and $S(CH_2)_{11}SO_3^-$. We prepared the mixed SAMs by soaking gold electrodes in solutions containing mixtures of $HS(CH_2)_{11}N^+(CH_3)_3$ and $HS(CH_2)_{11}SO_3^-$ with a mole fraction of $HS(CH_2)_{11}SO_3^-$ *in solution* $\chi^{sol}(SO_3^-) = 0.02$, 0.05, 0.1, 0.15, 0.2, 0.3, 0.5, 0.7, 0.8, and 0.9. We *assume* the mole fraction of the SO_3^--terminated SAM correlates (probably nonlinearly) with the composition in solution, but we have not measured this surface mole fraction experimentally. Figure 4a compares the cyclic voltammograms of cyt *c* adsorbed on the mixed SAMs of $\chi^{sol}(SO_3^-) = 0.02$ and 0.1 and a homogeneous SAM of $S(CH_2)_{11}N^+(CH_3)_3$. We observed significant change in the cathodic-to-anodic peak separations from $\chi^{sol}(SO_3^-) = 0$ to 0.02 but relatively little change from $\chi^{sol}(SO_3^-) = 0.02$ to 0.1. The cyclic voltammograms of cyt *c* adsorbed on mixed SAMs of $\chi^{sol}(SO_3^-) = 0.15$, 0.2, 0.3, 0.5, 0.7, 0.8, and 0.9 (not shown) show very weak or no electrochemical signals.

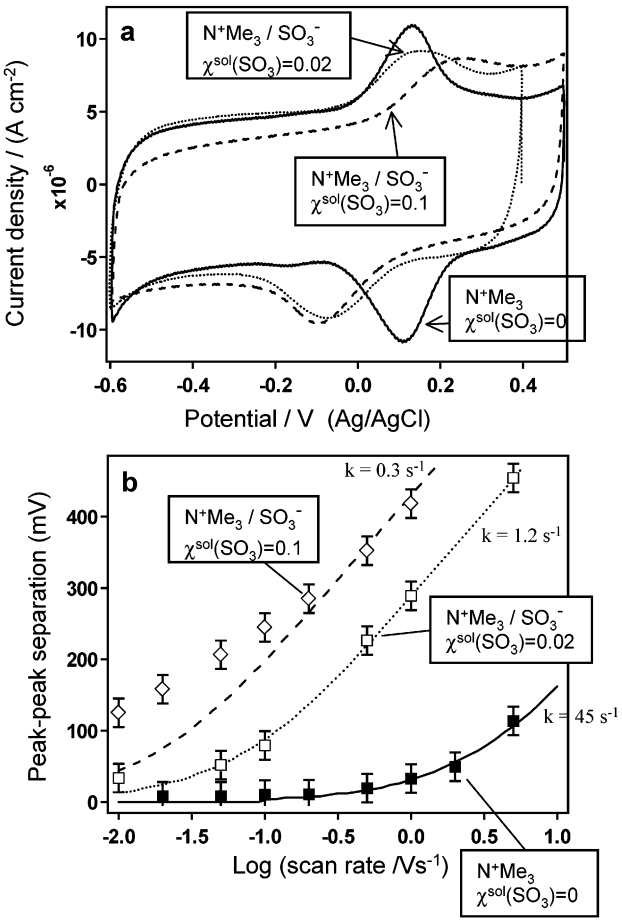

Figure 4. (a) Cyclic voltammograms of cyt *c* adsorbed on a homogeneous SAM of $S(CH_2)_{11}N^+(CH_3)_3$ (solid line), a mixed SAM prepared from a solution mixture of $HS(CH_2)_{11}N^+(CH_3)_3$ and $HS(CH_2)_{11}SO_3^-$ with $\chi^{sol}(SO_3^-) = 0.02$ (dotted line), and with $\chi^{sol}(SO_3^-) = 0.10$ (dashed line). Voltammetric scan rate: 0.5 V/s. (b) Plots of the anodic-to-cathodic peak separations as a function of the logarithmic of voltammetric scan rate. The anodic-to-cathodic peak separations were obtained from cyclic voltammograms of cyt *c* adsorbed on a homogeneous SAM of $S(CH_2)_{11}N^+(CH_3)_3$ (filled squares), a mixed SAM prepared from a solution mixture of $HS(CH_2)_{11}N^+(CH_3)_3$ and $HS(CH_2)_{11}SO_3^-$ with $\chi^{sol}(SO_3^-) = 0.02$ (open squares), and with $\chi^{sol}(SO_3^-) = 0.10$ (rhombuses). Homogeneous error bars of ±0.02 V were estimated to account for the uncertainty in peak measurements. The measured data are fitted to the theoretical curves (lines) using a locally written computer program based on Butler–Volmer electron-transfer theory. The corresponding electron-transfer rate constants used to calculate the curves are 45 s^{-1} (solid line), 1.2 s^{-1} (dotted line), and 0.3 s^{-1} (dashed line).

The major change in cyclic voltammogram from $\chi^{sol}(SO_3^-) = 0$ to 0.02 suggests that the mole fractions of the $N^+(CH_3)_3$ and SO_3^- groups on the surface do not correspond to the mole fraction of the thiols in the solution used to prepare the SAM. The mole fraction of the SO_3^- group on the surface is probably much larger than 0.02 when $\chi^{sol}(SO_3^-) = 0.02$. Although we have not measured the mole fraction of SO_3^- group on the surface, we observed

that an increase in the surface density of SO_3^- groups leads to an increase in cathodic-to-anodic peak separations for small values of $\chi^{sol}(SO_3^-)$. The increase in cathodic-to-anodic peak separations is a clear indication of the decrease in electron-transfer rates.

To obtain rate constants for electron transfer between the electrode and the heme of the adsorbed cyt *c*, we analyzed cyclic voltammograms obtained at a range of voltammetric scan rates. Figure 4b plots the anodic-to-cathodic peak separations as a function of the logarithm of the voltammetric scan rate (V s^{-1}) for cyt *c* adsorbed on the mixed SAMs of $\chi^{sol}(SO_3^-) = 0.02$ and 0.1 and a homogeneous SAM of $S(CH_2)_{11}N^+(CH_3)_3$. These data are fitted to the theoretical curves using a locally written computer program based on Butler−Volmer electron transfer theory.[47,52] We estimate the electron-transfer rate constant k_{ET}^0 of cyt *c* adsorbed on the homogeneous SAM terminated with $N^+(CH_3)_3$ groups to be 45 s^{-1} and k_{ET}^0 of cyt *c* adsorbed on the mixed SAM derived from the solution having $\chi^{sol}(SO_3^-) = 0.02$ to be 1.2 s^{-1}. The data for $\chi^{sol}(SO_3^-) = 0.1$ do not fit the theoretical curves well. In particular, the anodic-to-cathodic peak separations are still significantly large at slow voltammetric scans, indicating irreversible redox reactions at slow scan rate. The values of the anodic-to-cathodic peak separations at higher scan rate were fitted to theoretical curves to yield an estimated electron-transfer rate constant of 0.3 s^{-1}. The decrease in electron-transfer rate constant with the increase in the value of $\chi^{sol}(SO_3^-)$ suggests that the orientation of the protein changes when SO_3^- groups are introduced into a SAM terminating in NMe_3^+ groups.

We also observed that the redox potential of cyt *c* adsorbed on the mixed SAM ($\chi^{sol}(SO_3^-) = 0.1$) is 0.09 V vs Ag/AgCl, a value very close to the formal redox potential, while the redox potential of cyt *c* adsorbed on the homogeneous SAM of $S(CH_2)_{11}N^+(CH_3)_3$ is 0.13 V, slightly shifted from the standard potential. We hypothesize that the positively charged $N^+(CH_3)_3$ groups cause the redox potential to shift to a more positive value (more easily reduced), while, for proteins adsorbed on the mixed SAM, the presence of the negatively charged SO_3^- groups neutralize this electrostatic effect. Another possible reason for the disappearance of the shift in potential in the case of the mixed SAM might be a change in the orientation of the protein. This change might turn the heme away from the surface and result in a weaker influence of the positive charges of the $N^+(CH_3)_3$ groups in the redox behavior of the heme than in the case of pure $N^+(CH_3)_3$ surfaces.

When the value of $\chi^{sol}(SO_3^-) = 0.5$, we assume that the surface becomes zwitterionic and overall charge neutral. This surface has been established using SPR to resist protein adsorption.[29] The lack of electrochemical signal for $\chi^{sol}(SO_3^-) = 0.5$ is consistent with the SPR results.

Mixed SAMs of $S(CH_2)_{11}N^+(CH_3)_3$ and $S(CH_2)_{11}CH_3$. We have prepared the mixed SAMs by soaking gold electrodes in mixed solutions of $HS(CH_2)_{11}N^+(CH_3)_3$ and $HS(CH_2)_{11}CH_3$ with a mole fraction of $HS(CH_2)_{11}CH_3$ $\chi^{sol}(CH_3) = 0.1$, 0.15, 0.2, 0.25, 0.3, 0.35, 0.4, 0.5, 0.7, and 0.9. We observed cyclic voltammograms similar to the one shown in Figure 2a for the mixed SAMs of $\chi^{sol}(CH_3) = 0.1$ and 0.15, cyclic voltammograms with no observable redox peaks for the mixed SAMs of $\chi^{sol}(CH_3) = 0.2$, 0.25, 0.3, and 0.35, and cyclic voltammograms similar to the one shown in Figure 2c for the mixed SAMs of $\chi^{sol}(CH_3) = 0.4$, 0.5, 0.7, and 0.9. SPR suggests that there is a monolayer of cyt *c* molecules adsorbed on the mixed SAMs of $\chi^{sol}(CH_3) = 0.2$ even though there was no electrochemical signal. We infer that this absence of an electrochemical signal corresponds to a protein conformation or orientation unfavorable for electron transfer.

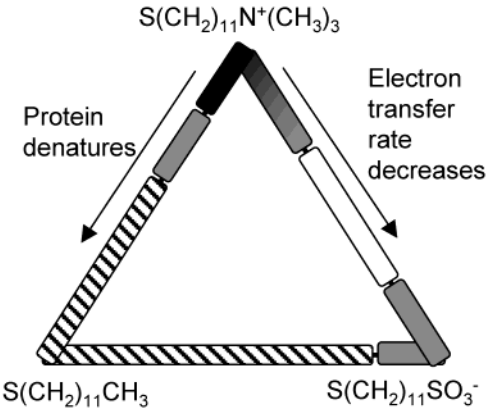

Figure 5. Diagram summarizes the variation in redox properties of cyt *c* adsorbed on mixed SAMs of $S(CH_2)_{11}N^+(CH_3)_3$, $S(CH_2)_{11}SO_3^-$, and $S(CH_2)_{11}CH_3$. Black indicates that protein conformation is preserved and fast electron transfer demonstrated, gray indicates no electron transfer observed for adsorbed proteins, the gradient of black to gray represents the transition between fast and slow electron transfer, stripes indicates that the protein is denatured, and white indicates that no protein is adsorbed on the surface. For mixed SAMs of $S(CH_2)_{11}N^+(CH_3)_3$ and $S(CH_2)_{11}SO_3^-$, we observed rates of electron transfer from fast to slow for $\chi^{sol}(SO_3^-) = 0$, 0.02, 0.05, and 0.1, a very weak electrochemical signal for $\chi^{sol}(SO_3^-) = 0.15$ and 0.2, and no electrochemical signal for $\chi^{sol}(SO_3^-) = 0.3$, 0.5, 0.7, 0.8, 0.9, and 1. SPR measurements suggest that a full monolayer of protein was adsorbed for $\chi^{sol}(SO_3^-) = 0$, less than 5% of a monolayer of protein adsorbed for $\chi^{sol}(SO_3^-) = 0.3$, 0.5, and 0.7, and a double layer of protein adsorbed for $\chi^{sol}(SO_3^-) = 1$. For the mixed SAMs of $S(CH_2)_{11}N^+(CH_3)_3$ and $S(CH_2)_{11}CH_3$, we observed the same potential and electron-transfer rate for $\chi^{sol}(CH_3) = 0$, 0.1, and 0.15, very weak electrochemical signals for $\chi^{sol}(CH_3) = 0.2$, 0.25, 0.3, and 0.35, and denatured cyt *c* for $\chi^{sol}(CH_3) = 0.4$, 0.5, 0.7, and 1. SPR measurements suggest that a full monolayer of protein was adsorbed for $\chi^{sol}(CH_3) = 0$, 0.2, and 1. For the mixed SAMs of $S(CH_2)_{11}CH_3$ and $S(CH_2)_{11}SO_3^-$, we observed denatured cyt *c* for $\chi^{sol}(SO_3^-) = 0$, 0.3, 0.5, and 0.7 and no electrochemical signal for $\chi^{sol}(SO_3^-) = 0.9$ and 1.

Figure 5 summarizes the variation of the redox properties of cyt *c* adsorbed on mixed SAMs of $S(CH_2)_{11}N^+(CH_3)_3$, $S(CH_2)_{11}SO_3^-$, and $S(CH_2)_{11}CH_3$.

Conclusions

This paper shows that trimethylammonium-terminated SAMs adsorb approximately a monolayer of cyt *c* in a conformation that allows rapid exchange of electrons between its heme group and the electrode. This surface may have advantages over the carboxyl-terminated SAMs for studies of cyt *c* electrochemistry, since the electrochemistry of cyt *c* adsorbed on carboxyl-terminated SAMs is often complicated by protonation and deprotonation of the carboxyl groups.[44−46]

More broadly, the paper demonstrates that SAMs provide a sensitive way to control orientation and conformation of a representative small protein—cyt *c*—on a surface. By using different SAM, one can get a wide range of behaviors, from behavior similar to solution to complete denaturation. This kind of control is useful in the design of biomaterials, biosensors, and bioanalytical systems.[1,2] The clear influence of the structure of the SAM on the electrochemical behavior of cyt *c* adsorbed on it suggests that electrochemistry can serve as a valuable tool for

(52) Tender, L.; Carter, M. T.; Murray, R. W. *Anal. Chem.* **1994**, *66*, 3173−3181.

investigating the conformation of this protein (and perhaps others) on the surface of electrodes.

This study provides a probe that can be used to study interactions of cyt *c*—a representative small protein—with a broad range of surfaces. Electrochemistry of cyt *c* on SAMs is thus a new probe for surface−protein interaction that complements SPR and quartz crystal microbalance (QCM) in that it gives information about orientation and conformation. It also gives a new degree of control over a system widely used to study electron transfer in proteins. By incorporating components that are electroactive, this method can probably be used to examine electron transfer through thin organic films.[53−57]

Experimental Section

Materials. All chemicals used were reagent grade unless stated otherwise. Horse heart cytochrome *c* (Sigma no. C7752), yeast cytochrome *c* (Sigma no. C2436), and sodium dodecyl sulfate were purchased from Sigma (St. Louis, MO) and used as received. 1-Dodecanethiol was purchased from TCI American (Portland, OR). Absolute ethanol was purchased from Pharmco Products (Brookfield, CT). Alkanethiols $Na[HS(CH_2)_{11}SO_3]$ and $[HS(CH_2)_{11}N(CH_3)_3]Cl$ were synthesized as previously described.[33]

Buffers and Solutions of Proteins. We used buffers with the following compositions: (A) 4.4 mM potassium phosphate, pH 7.4, ionic strength (μ) = 10 mM;[58] (B) 0.44 mM potassium phosphate, pH 7.4, μ = 1 mM. Buffers were prepared in Nanopure water. Solutions of protein were prepared by dissolving solid protein in the buffer B at a concentration of 1 mg/mL at room temperature. Cyt *c* from Sigma was approximately 90% pure (estimated by reverse-phase HPLC). We purified it further chromatographically on (carboxymethyl)cellulose (CM 32, Whatman) and then desalted using a NAP-25 column from Pharmacia Biotech and dialyzed for 4 h to equilibrate the buffer. The electrochemical results were similar for unpurified cyt *c* (directly from Sigma) and for purified cyt *c*: we infer that impurities are not responsible for the behavior we see.

Electrode Preparation. The working electrode was prepared by evaporation of titanium (10 Å) and gold (400 Å) onto glass slides. The electrodes were then incubated in various solutions prepared with the different alkanethiols used in this work. 1-Dodecanethiol was dissolved in ethanol, and $Na[HS(CH_2)_{11}SO_3]$ and $[HS(CH_2)_{11}N(CH_3)_3]Cl$ were dissolved in water at a concentration of 2 mM. Mixed SAMs are prepared by mixing freshly prepared ethanol or water solution of the corresponding alkanethiols. The incubation time was 24 h.

Electrochemical Measurements. The reference electrode was an Ag/AgCl electrode in 3 M KCl; the counter electrode was platinum mesh. Electrochemical measurements were performed using a classical three-electrode system and a potentiostat (model AFCBP1) from Pine Instrument Co. (Grove City, PA). Cyclic voltammograms were not IR compensated. The electrolyte solution is buffer A. The SAM-modified electrodes were first used to obtain a background voltammogram and then incubated in a solution of cyt *c* for 30 min. The cyclic voltammograms were then recorded.

Surface Plasmon Resonance Spectroscopy. SPR was performed on a Biacore 1000 instrument (Biacore). The substrate containing the SAM to be analyzed was mounted in a SPR cartridge as previously described. Our SPR protocol for measuring the adsorption of protein to SAMs consisted of the following: (i) flowing buffer A for 2 min, then replacing the flow of buffer with a flow of a solution of protein (1 mg/mL in buffer B) for 30 min, and finally injecting buffer A for an additional 10 min; (ii) flowing a solution of sodium dodecyl sulfate (40 mM in buffer A) over the SAM surface for 15 min followed by rinsing the surface with buffer A for 5 min. The flow rate used for all experiments was 10 μL/min.

Acknowledgment. This work was supported by the NIH (Grant GM30367). R.F. is grateful to the Swiss National Science Foundation for a postdoctoral fellowship.

LA0204794

(53) Chidsey, C. E. D. *Science* **1991**, *251*, 919−922.
(54) Dubois, L. H.; Nuzzo, R. G. *Annu. Rev. Phys. Chem.* **1992**, *43*, 437−463.
(55) Sachs, S. B.; Dudek, S. P.; Hsung, R. P.; Sita, L. R.; Smalley, J. F.; Newton, M. D.; Feldberg, S. W.; Chidsey, C. E. D. *J. Am. Chem. Soc.* **1997**, *119*, 10563−10564.
(56) Haas, A. S.; Pilloud, D. L.; Reddy, K. S.; Babcock, G. T.; Moser, C. C.; Blasie, J. K.; Dutton, P. L. *J. Phys. Chem. B* **2001**, *105*, 11351−11362.
(57) Chen, X.; Discher, B. M.; Pilloud, D. L.; Gibney, B. R.; Moser, C. C.; Dutton, P. L. *J. Phys. Chem. B* **2002**, *106*, 617−624.
(58) Collinsen, M.; Bowden, E. F. *Langmuir* **1992**, *8*, 1247−1250.